ELSEVIER

www.elsevier.nl/locate/jorganchem

Journal of Organometallic Chemistry 601 (2000) 69–77

Journal of Organometallic Chemistry

Synthesis and molecular structure of $[RuCl\{C(=CHPh)OC(=O)CH_2CH_3\}(CO)(PPh_3)_2]$: a real intermediate in ruthenium complex-catalyzed selective synthesis of a (*Z*)-enol ester

Hiroyuki Kawano [a,*], Yoshiko Masaki [b], Takahiro Matsunaga [b], Katsuma Hiraki [b], Masayoshi Onishi [b], Taro Tsubomura [c]

[a] *Graduate School of Marine Science and Engineering, Nagasaki University, Bunkyo-machi, Nagasaki 852–8521, Japan*
[b] *Department of Applied Chemistry, Faculty of Engineering, Nagasaki University, Bunkyo-machi, Nagasaki 852–8521, Japan*
[c] *Department of Industrial Chemistry, Faculty of Engineering, Seikei University, Kichijoji, Musashinoshi, Tokyo 180-8633, Japan*

Received 4 October 1999; received in revised form 4 January 2000; accepted 14 January 2000

Abstract

Reaction of $[RuCl(\eta^2\text{-}O_2CCH_2CH_3)(CO)(PPh_3)_2]$ (**1**) and phenylacetylene gives $[RuCl\{C(=CHPh)OC(=O)CH_2CH_3\}(CO)(PPh_3)_2]$ (**2a**). The X-ray structure analysis of **2a** reveals that it includes a (*Z*)-enol ester-like 1-propanoyloxy-2-phenylethenyl-C^1,*O* ligand. In the catalytic addition of propanoic acid to phenylacetylene, the complex **2a** acts as a real intermediate that gives (*Z*)-2-phenylethenyl propanoate, selectively. The presence of the free PPh_3 in the reaction mixture depresses formation of some dicarbonylruthenium species that catalytically produce (*E*)- and Markovnikov-type enol esters. © 2000 Elsevier Science S.A. All rights reserved.

Keywords: Ruthenium complexes; Selective catalysis; Catalytic intermediate; Enol ester; X-ray structure

1. Introduction

Direct addition of carboxylic acids to terminal alkynes with the aid of transition-metal complexes is a powerful tool for preparing synthetically useful enol esters [1] (see Scheme 1). In 1985, Mitsudo and Watanabe's group [2] and Dixneuf's group [3] independently achieved the direct addition under mild conditions using ruthenium complexes as catalysts. In most cases, the catalytic addition promoted by the ruthenium complexes affords the Markovnikov-type products, selectively. Dixneuf and collaborators have applied the ruthenium-catalyzed Markovnikov addition to the one-pot syntheses of 2-acyloxy-1,3-dienes [4], enol formates [5], and chiral 1,3-dioxolan-4-ones [6]. As for the (*E*)-type products, the presence of phosphine ligands in the catalytic system generally leads to the regioselective formation [2,7]. However, in contrast, it is reported rarely that the catalytic addition affords a (*Z*)-type enol ester, regioselectively. Addition of benzoic acid onto 1-hexyne catalyzed by $[Ru(\eta^3\text{-}C_4H_7)_2(dppe)]$ reported by Dixneuf's group [8] is the first example of the selective synthesis of (*Z*)-enol esters. Very recently, Matas et al. [9] have reported the second (*Z*)-selective addition of ferrocenecarboxylic acid to phenylacetylene. These two works, however, have shown no reason why the (*Z*)-enol esters are produced predominantly in their catalytic systems and gave no information about the intermediary organometallic species.

From the viewpoint of organometallic complexes, on the other hand, there have been some organoruthenium complexes closely related to the catalytic formation of enol esters reported. Daniel et al. [10] and Esteruelas et al. [11] have independently synthesized a new class of ruthenium(II) complexes having the enol ester-like 2-substituted-1-acyloxyethenyl chelate ligands. In spite of

* Corresponding author. Tel.: +81-95-8437281; fax: +81-95-8476749.
E-mail address: hirokwn@net.nagasaki-u.ac.jp (H. Kawano)

PII: S0022-328X(00)00027-9

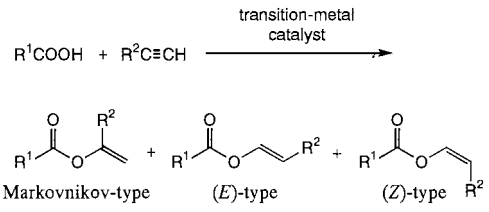

Scheme 1. Transition-metal-catalyzed direct addition of a carboxylic acid to a terminal alkyne producing the three types of enol esters.

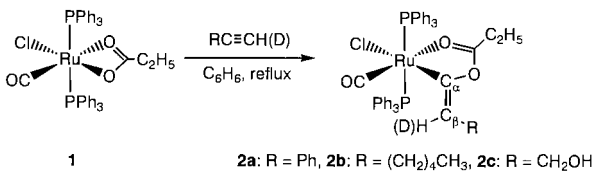

Scheme 2. Production of **2a**–**c** bearing the (*Z*)-enol ester-like chelate ligand.

the structures of the chelating ligands, they have not reported the catalytic aspects of their complexes. Hence, there still exists a missing link between the possible intermediary organometallic species and the catalytic regioselective synthesis of (*Z*)-enol esters.

Here we report the reactions of a propanoatoruthenium(II) complex, $[RuCl(\eta^2\text{-}O_2CCH_2CH_3)(CO)(PPh_3)_2]$ (**1**), with some terminal alkynes producing a series of novel ruthenium(II) complexes, $[RuCl\{C(=CHR)O\text{-}C(=O)CH_2CH_3\}(CO)(PPh_3)_2]$ (R = Ph for **2a**, R = $(CH_2)_4CH_3$ for **2b**, and R = CH_2OH for **2c**) bearing 2 - substituted - 1 - propanoyloxyethenyl - C^1,O - chelates, namely, the (*Z*)-enol ester-like ligands (Scheme 2). The molecular structure of **2a** is determined by single-crystal X-ray analysis. Moreover, the complex is found to be a real intermediate in the catalytic synthesis of the (*Z*)-enol ester; detailed studies reveal the missing link and the overall reaction pathways of the catalytic addition of propanoic acid to phenylacetylene producing the (*Z*)-enol ester, regioselectively.

2. Experimental

All experiments were performed under a dry nitrogen atmosphere using standard Schlenk tube techniques. However, any special precautions against air and moisture were not taken in handling the complexes, since most of the complexes were air-stable as solids and stable for a short period in solution. All solvents were dried and distilled over appropriate drying agents and stored under nitrogen before use. The complex $[RuClH(CO)(PPh_3)_3]$ (**3**) was prepared according to the literature [12]. Phenylacetylene-d_1 was prepared by treating a solution of sodium phenylacetylide with D_2O in diethyl ether. All other reagents were purchased and used without further purification unless otherwise stated.

Infrared spectra were recorded on a JASCO A-100 spectrometer using KBr tablets. GLPC analyses were carried out on a Hitachi model 263-30 equipped with a flame ionization detector and a 5 mmϕ × 3 m stainless-steel column (SE-30 or PEG 20M). NMR spectra were obtained on a JEOL GX-400 spectrometer operating at 400 MHz for ^{1}H, 101 MHz for ^{13}C referenced to $Si(CH_3)_4$, and at 162 MHz for ^{31}P referenced to 85% H_3PO_4 in water. Elemental analyses were performed on a Yanaco MT-3 CHN Recorder and FABMS measurements on a JEOL JMS-DX303 mass spectrometer at the Center for Instrumental Analysis, Nagasaki University.

2.1. Preparation of *1*

Preparation of **1** was carried out in a modified manner according to the reported procedure [13]. A mixture of **3** (1.06 g, 1.11 mmol) and propanoic acid (1.51 g, 20.4 mmol) in benzene (30 ml) was refluxed for 24 h under nitrogen. After the reaction, the reaction mixture was concentrated under a reduced pressure. A small amount of the *cis*-isomer and propanoic acid were removed from the crude product by silica-gel column chromatography (eluent: CH_2Cl_2). The complex **1** was isolated after CH_2Cl_2 was removed (yield 0.64 g, 75%). Anal. Calc. for $C_{40}H_{35}ClO_3P_2Ru$: C, 63.03; H, 4.63. Found: C, 63.32; H, 5.15%.

2.2. Preparation of *[RuCl{C(=CHPh)OC(=O)CH$_2$CH$_3$}(CO)(PPh$_3$)$_2$] (2a)*

A mixture of **1** (214 mg, 0.28 mmol) and phenylacetylene (0.47 g, 4.6 mmol) in benzene (20 ml) was refluxed for 3 h under nitrogen. The yellow–orange suspension turned smoothly into a solution. The reaction mixture was concentrated to 1/4–1/5 of its original volume under a reduced pressure. Addition of hexane to the concentrated reaction mixture gave a crude **2a** as a yellow powder. Then the crude **2a** was applied to the silica-gel column chromatography using benzene–dichloromethane (4:1) as eluent. Evaporation of the eluent gave **2a** in a pure form, as a dichloromethane solvate (yield 186 mg, 63%). No satisfactory microanalysis data have been obtained since the incorporated dichloromethane is released readily even at room temperature (r.t.). M.p. (dec.) 187–189°C. IR (cm^{-1}): ν(C≡O) 1935 vs, ν(C=O) 1630 vs, ν(C=C) 1597 s. ^{1}H-NMR ($CDCl_3$): δ 0.64 (t, 3H, J(HH) = 7.5 Hz, CH_3), 1.80 (q, 2H, J(HH) = 7.5 Hz, CH_2), 4.41 (s, 1H, C*H*), 6.72 (d, 2H, J(HH) = 7.3 Hz, *o*-*H* on the chelate ligand), 6.97 (t, 1H, J(HH) = 7.3 Hz, *p*-*H* on the chelate ligand), 7.10 (t, 2H, J(HH) = 7.3 Hz, *m*-*H* on the chelate ligand), 7.25 (m, 18H, *p*- and *m*-*H* on the PPh_3), 7.61 (m, 12H, *o*-*H* on the PPh_3). ^{13}C{^{1}H}-NMR ($CDCl_3$): δ 8.3 (s, CH_3), 25.5 (s, CH_2), 121.1 (s, C_β),

127.8 (s), 129.7 (s), 130.7 (t, J(CP) = 21.5 Hz), 134.6 (s), 181.1 (s, CO_2), 188.6 (t, J(CP) = 13.6 Hz, C_α), 204.8 (t, J(CP) = 15.6 Hz, C≡O). $^{31}P\{^1H\}$-NMR ($CDCl_3$): δ 33.6 (s).

2.3. Reaction of **1** with phenylacetylene-d_1

A solution of **1** (101 mg, 0.13 mmol) and phenylacetylene-d_1 (0.78 g, 7.6 mmol) in benzene (20 ml) was allowed to react under reflux. After 3 h, the solvent was removed under a reduced pressure. The non-volatile residue was dissolved to $CDCl_3$ (0.5 ml) and applied to NMR measurements. The $^{31}P\{^1H\}$-NMR spectrum showed that the entire starting complex was converted into **2a**-d_1 (δ 33.6 (s)). The loss of the ^{1}H-signal at δ 4.41 and the splitting of the $^{13}C\{^1H\}$-signal at δ 121.1 (J(CD) = 36 Hz) into three peaks indicated that the β-carbon of the chelating ligand was deuterated. No other significant change was found in the NMR spectra.

2.4. Preparation of *[RuCl{C(=CHC$_5$H$_{11}$)OC(=O)CH$_2$CH$_3$}(CO)(PPh$_3$)$_2$]* (**2b**)

A mixture of **1** (75 mg, 0.10 mmol) and 1-heptyne (96 mg, 1.0 mmol) in benzene (25 ml) was refluxed for 72 h under nitrogen. After the reaction was over, a similar work-up procedure for **2a** gave the complex **2b** as a yellow powder (yield 53 mg, 63%). Anal. Calc. for $C_{47}H_{47}ClO_3P_2Ru$: C, 65.77; H, 5.52. Found: C, 65.65; H, 5.80%. m.p. (dec.) 221–223°C. IR (cm^{-1}): ν(C≡O) 1935 vs, ν(C=O) 1635 vs, ν(C=C) 1610 s. ^{1}H-NMR ($CDCl_3$): δ 0.54 (t, 3H, J(HH) = 7.3 Hz, CH_3), 0.81 (m, 2H, CH_2), 0.82 (t, 3H, J(HH) = 7.3 Hz, CH_3), 0.98 (m, 2H, CH_2), 1.16 (m, 2H, CH_2), 1.63 (m, 4H, 2CH_2), 3.51 (tt, 1H, J(HH) = 5.8 Hz, J(HP) = 2.2 Hz, CH), 7.34 (m, 18H, p- and m-H on the PPh_3), 7.65 (m, 12H, o-H on the PPh_3). $^{13}C\{^1H\}$-NMR ($CDCl_3$): δ 8.4 (s, CH_3), 14.1 (s, CH_3), 22.6 (s, CH_2), 25.4 (s, CH_2), 27.3 (s, CH_2), 29.1 (s, CH_2), 31.8 (s, CH_2), 121.3 (s, C_β), 127.7 (s), 129.6 (s), 131.6 (t, J(CP) = 21.5 Hz), 134.6 (s), 179.0 (t, J(CP) = 13.7 Hz, C_α), 180.6 (s, CO_2), 205.4 (t, J(CP) = 13.7 Hz, C≡O). $^{31}P\{^1H\}$-NMR ($CDCl_3$): δ 33.9 (s).

2.5. Reaction of 2-propyn-1-ol with **1** producing *[RuCl{C(=CHCH$_2$OH)OC(=O)CH$_2$CH$_3$}(CO)(PPh$_3$)$_2$]* (**2c**)

A mixture of **1** (76 mg, 0.10 mmol) and 2-propyn-1-ol (30 mg, 0.54 mmol) in benzene (30 ml) was refluxed for 20 h under nitrogen. Addition of hexane to the concentrated reaction mixture gave a crude **2c** as a yellow powder (yield 50 mg). Unfortunately, any effort to get the pure **2c** out of the crude product resulted in failure. The identification of **2c** was achieved using IR and NMR spectroscopic methods. IR (cm^{-1}): ν(C≡O) 1935 vs, ν(C=O) 1625 vs, ν(C=C) 1600 sh. ^{1}H-NMR ($CDCl_3$): δ 0.63 (t, 3H, J(HH) = 7.6 Hz, CH_3), 1.84 (q, 2H, J(HH) = 7.6 Hz, CH_2), 3.50 (m, 2H, CH_2), 3.75 (tt, 1H, J(HH) = 7.0, J(HP) = 1.9 Hz, CH), 7.36 (m, 18H, p- and m-H on the PPh_3), 7.71 (m, 12H, o-H on the PPh_3). $^{13}C\{^1H\}$-NMR ($CDCl_3$): δ 8.2 (s, CH_3), 25.4 (s, CH_2), 58.0 (s, CH_2), 119.1 (s, C_β), 127.8 (s), 129.8 (s), 131.5 (t, J(CP) = 21.5 Hz), 134.7 (s), 180.9 (s, CO_2), 187.0 (t, J(CP) = 13.6 Hz, C_α), 204.6 (t, J(CP) = 15.6 Hz, C≡O). $^{31}P\{^1H\}$-NMR ($CDCl_3$): δ 32.8 (s).

2.6. Acidolysis of **2a** producing the dicarbonylruthenium(II) complexes

A solution of **2a** (44 mg, 0.051 mmol) and propanoic acid (25 mg, 0.34 mmol) in benzene (5 ml) was allowed to react in a sealed tube at 80°C. After 24 h, a small portion of the mixture was analyzed by GLPC. The GLPC analysis showed a peak of (*Z*)-PhCH=CHOC(=O)CH$_2$CH$_3$; no peak due to the (*E*)- or Markovnikov-type enol esters was detected. The rest of the mixture was concentrated under a reduced pressure, dissolved in C_6D_6 (0.5 ml) and applied to NMR analysis. The $^{31}P\{^1H\}$-NMR spectrum showed four singlets: δ 34.4 (**1**, 20%), 31.8 (14%), 24.1 (50%), and 15.4 (16%), relative intensities shown in parentheses. The last three signals were assigned to the following dicarbonylruthenium(II) complexes, [Ru{η^1-OC(=O)C$_2$H$_5$}$_2$(CO)$_2$(PPh$_3$)$_2$] (**4**), [RuCl{η^1-OC(=O)C$_2$H$_5$}(CO)$_2$(PPh$_3$)$_2$] (**5**), and *cct*-[RuCl$_2$(CO)$_2$(PPh$_3$)$_2$] (**6**) [14], respectively. The identification of the novel dicarbonyl complexes **4** and **5** was achieved by comparing their NMR data to those of the authentic samples prepared according to the literature method [15]. The NMR spectroscopic data for **4**, ^{1}H-NMR (C_6D_6): δ 0.87 (t, 6H, J(HH) = 7.3 Hz, CH_3), 1.83 (q, 4H, J(HH) = 7.3 Hz, CH_2), 7.00 (m, 6H, p-H), 7.09 (m, 12H, m-H), 8.04 (m, 12H, o-H). $^{31}P\{^1H\}$-NMR (C_6D_6): δ 31.8 (s). The NMR spectroscopic data for **5**, ^{1}H-NMR (C_6D_6): δ 0.93 (t, 3H, J(HH) = 7.7 Hz, CH_3), 1.94 (q, 2H, J(HH) = 7.7 Hz, CH_2), 6.97 (m, 6H, p-H), 7.04 (m, 12H, m-H), 8.10 (m, 12H, o-H). $^{31}P\{^1H\}$-NMR (C_6D_6): δ 24.1 (s).

2.7. Catalytic addition of propanoic acid to phenylacetylene forming the enol esters

A mixture of a catalyst precursor (0.10 mmol), propanoic acid (10 mmol), phenylacetylene (10 mmol), triphenylphosphine (0.10 mmol, if required) and undecane (an internal standard, 2.8 mmol) in benzene (10 ml) was placed in a reaction vessel equipped with a reflux condenser and a rubber septum. The mixture was refluxed under a nitrogen atmosphere. At appropriate

intervals, a small portion of the reaction mixture was sampled through the septum and applied to GLPC analysis. Yields of the enol esters were given by means of the GLPC analysis of the reaction mixture.

In order to follow the ruthenium-containing species in the catalytic system, the catalyst precursor (0.02 mmol), propanoic acid (0.80 mmol), and phenylacetylene (0.80 mmol) in C_6D_6 (0.6 ml) were sealed under vacuum in an NMR tube. The reaction tube was heated at 80°C. After an appropriate reaction time, the reaction was stopped by cooling the tube in an ice bath, then the NMR spectra of the reaction mixture were measured at 30°C.

2.8. X-ray structure study of **2a**·$2CH_2Cl_2$

Recrystallization of **2a** from dichloromethane–hexane solution afforded single crystals suitable for X-ray diffraction structure analysis. Dichloromethane was incorporated as crystallizing solvent in the crystal. Crystal data for **2a**·$2CH_2Cl_2$: $C_{48}H_{41}ClO_3P_2Ru\cdot 2CH_2Cl_2$, $M = 1034.19$, monoclinic, space group $P2_1/m$ (no. 11); $a = 9.805(1)$, $b = 22.688(2)$, $c = 11.406(2)$ Å; $\beta = 107.754(9)°$; $V = 2416.4$ Å^3; $Z = 2$; yellow prism $0.35 \times 0.35 \times 0.50$ mm; $\mu(\text{Mo}-\text{K}_\alpha) = 7.07$ cm^{-1}. The intensity data were collected at 20°C on a Rigaku AFC5S diffractometer with graphite-monochromated Mo–K_α radiation [$\lambda(\text{Mo}-\text{K}_\alpha) = 0.71069$ Å]. The ω–2θ scan technique was applied with a maximum 2θ value of 60.0°. Of the 7606 reflections that were collected, 7230 were unique ($R_{\text{int}} = 0.035$). The intensities of three standard reflections, measured every 150 reflections throughout the data collection, decayed by 2.18%, and a linear correction factor was applied. The intensities were corrected for Lorentz and polarization effects. An empirical absorption correction based on azimuthal scans of several reflections was applied (transmission factors in the range 0.95–1.00). The structure was solved by heavy-atom Patterson methods [16] and expanded using Fourier techniques [17]. All non-hydrogen atoms were refined anisotropically. Hydrogen atoms were included but not refined. Possible disorder of C29 was neglected and it was positioned on the crystallographic symmetry plane according to the restriction of the space group. The final structure apparently included some errors arising from fixing C29 on the symmetry plane. Nevertheless, the errors never affected our discussion of the structure of the chelating ligand so much. The final cycle of full-matrix least-squares refinement was based on 3073 observed reflections [$I > 3\sigma(I)$] and 304 variable parameters. The function minimized was $\Sigma\, w(|F_o| - |F_c|)^2$. Final R and R_w values were 0.055 and 0.039, respectively $\{R = \Sigma\||F_o| - |F_c|\|/\Sigma|F_o|$, $R_w = [\Sigma\, w(|F_o| - |F_c|)^2/\Sigma\, wF_o^2]^{1/2}$, where $w^{-1} = \sigma^2(F_o) + 0.006(F_o)^2\}$. Goodness-of-fit factor was 1.68. All calculations were performed using the TEXSAN [18] crystallographic software package.

3. Results and discussion

3.1. Reaction between [RuCl(η^2-$O_2CCH_2CH_3$)(CO)(PPh_3)$_2$] (**1**) and terminal alkynes giving 2-substituted-1-propanoyloxyethenyl-C^1,O-chelate ligands

The reactions of a propanoatoruthenium(II) complex, [RuCl(η^2-$O_2CCH_2CH_3$)(CO)(PPh_3)$_2$] (**1**) with some terminal alkynes gave a series of ruthenium(II) complexes bearing enol ester-like 2-substituted-1-propanoyloxyethenyl-C^1,O-chelate ligands. The reaction of **1** with phenylacetylene gave 1-propanoyloxy-2-phenylethenylruthenium(II) complex [RuCl{C(=CHPh)OC(=O)CH_2CH_3}(CO)(PPh_3)$_2$] (**2a**) as a yellow powder. The ^{1}H-NMR spectrum of **2a** contains a singlet at δ 4.41 due to the vinylic proton. Additionally, a characteristic set of ^{1}H-signals of an ethyl group indicates the presence of the propanoate moiety. The vinyl carbon atoms appear at δ 188.6 (triplet, J(CP) = 13.6 Hz, C_α) and 121.1 (C_β) in its ^{13}C{^{1}H}-NMR spectrum. Although the latter signal should have been observed as a triplet because of the P–C coupling, the coupling constant is too small to be observed in comparison with the resolution of our spectrometer (3.91 Hz). Actually, J(CP) values for closely related complexes have been reported to be 2–3 Hz by Esteruelas et al. [11]. The ^{1}H-^{13}C COSY-NMR spectrum suggests that the vinyl proton (δ 4.41) is attached to the C_β (δ 121.1). The ^{31}P{^{1}H}-NMR spectrum shows a singlet at δ 33.6, indicating that the two PPh_3 ligands are equivalent and positioned mutually *trans*. The IR spectrum of **2a** shows a ν(C≡O) vibration at 1935 cm^{-1}, a ν(C=O) at 1630 and a ν(C=C) at 1597.

Two other terminal alkynes, 1-heptyne and propargyl alcohol reacted with **1** to give the corresponding complexes, [RuCl{C(=CHC_5H_{11})OC(=O)CH_2CH_3}(CO)(PPh_3)$_2$] (**2b**) and [RuCl{C(=CHCH_2OH)OC(=O)CH_2-CH_3}(CO)(PPh_3)$_2$] (**2c**), respectively. These two complexes show common features in their NMR and IR spectroscopic data that indicate both **2b** and **2c** are the same class as **2a**. The signals of the ethyl group of the propanoate moiety, the vinyl proton and the two vinyl carbons give the formation of the chelating enol ester-like ligand.

Unfortunately, reaction of **1** with propargylamine gave a complicated mixture of products that were difficult to characterize. The elementary analysis and ^{31}P-NMR data of the mixture indicated a significant loss of the phosphorus content of the products. The nitrogen content, on the contrary, was larger than expected. A similar behavior was observed for the reaction of **1** and methyl propargyl sulfide. These results suggest that the exchange between the phosphine ligands and the amine (and also sulfide) is favored more

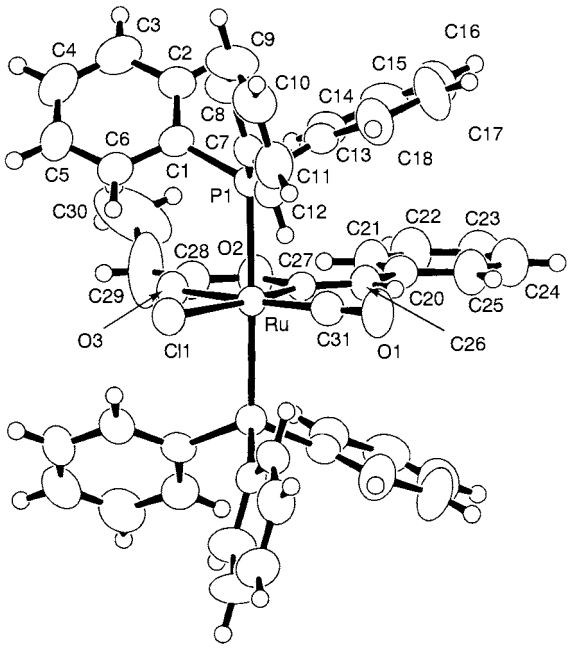

Fig. 1. The molecular structure of **2a** with the atom-numbering scheme. Dichloromethane molecules are omitted. The atom numbers in an asymmetric unit are indicated.

than the formation of the chelating ligand. On the other hand, treatment of **1** with diphenylacetylene, 1-phenyl-1-butyne or 4-octyne, under toluene refluxing conditions, resulted in the recovery of the starting complex. The internal triple bond never reacted with the propanoate **1**.

3.2. Molecular structure of *2a*

The single-crystal X-ray analysis of **2a** revealed an octahedral arrangement of the ligands around the ruthenium center. A perspective view of the molecular structure of **2a** is illustrated in Fig. 1. Selected bond lengths and angles are listed in Table 1. There exists a crystallographic symmetry plane including Ru atom in the molecule of **2a**. The CO, Cl and all non-hydrogen atoms in the chelating 1-propanoyloxy-2-phenylethenyl-C^1,O ligand except for the terminal CH_3 are positioned on the plane. Two positions of the disordered methyl group and those of two PPh_3 ligands are symmetrical about the same plane, respectively. The chelate ligand apparently shows its (*Z*)-enol ester-like backbone.

Some characteristic bond lengths of the chelating ligand inform us that the ligand is in resonance between the structures **A** and **B** shown in Scheme 3. Owing to the contribution of the resonance with the η^1-propanoato-η^1-phenylethenylideneruthenium(II) structure **B**, the Ru–C27 distance (2.007(8) Å) is similar to those of the related $[Ru(\eta^5\text{-}C_5H_5)\{C(=CHCO_2CH_3)OC(=O)CH_3\}(PPh_3)]$ (2.002(2) Å) [10] and $[Ru\{C(=CHPh)OC(=O)CH_3\}(CO)(acetone)(P^iPr_3)_2]BF_4$

Table 1
Selected bond lengths (Å) and angles (°) for **2a**·$2CH_2Cl_2$

Bond lengths	
Ru–Cl1	2.481(2)
Ru–P1	2.394(1)
Ru–O3	2.127(5)
Ru–C27	2.007(8)
Ru–C31	1.805(9)
O1–C31	1.156(9)
O2–C27	1.470(8)
O2–C28	1.328(10)
O3–C28	1.223(9)
C20–C26	1.46(1)
C26–C27	1.331(9)
C28–C29	1.51(1)
C29–C30	1.22(2)
Bond angles	
Cl1–Ru–P1	90.11(5)
Cl1–Ru–O3	88.7(2)
Cl1–Ru–C27	167.6(2)
Cl1–Ru–C31	100.2(3)
P1–Ru–O3	89.06(5)
P1–Ru–C27	89.69(5)
P1–Ru–C31	90.90(5)
O3–Ru–C27	78.9(3)
O3–Ru–C31	171.2(3)
C27–Ru–C31	92.2(3)
C27–O2–C28	115.8(7)
Ru–O3–C28	112.9(6)
C27–C26–C20	134.4(8)
Ru–C27–O2	110.6(5)
Ru–C27–C26	135.6(6)
O2–C27–C26	113.8(7)
O2–C28–O3	121.9(9)
O3–C28–C29	123.9(9)
C28–C29–C30	124(1)
Ru–C31–O1	176.4(8)

(1.967(8) Å) [11], and is shorter than those of the ordinary Ru–C_{sp^2} single bonds found in $[Ru(\eta^5\text{-}C_5H_5)\{C(=CHPh)O^iPr\}(CO)(PPh_3)]$ (2.103(6) Å) [19], $[Ru\{C(=CHCO_2CH_3)CO_2CH_3\}(CO)(NCCH_3)_2(PPh_3)_2]ClO_4$ (2.12(5) Å) [20], and $[Ru\{CH=CH^tBu\}Cl(CO)\{(CH_3)_2Hpz\}(PPh_3)_2]$ (2.063(7) Å) [21]. Additionally, the Ru–C27 distance is longer than most of the Ru=C_α distances (1.75–1.90 Å) of the reported ethenylideneruthenium(II) complexes [22] according to its partial double bonding character. The contribution of the structure **B** also weakens the C27–O2 bond; the bond

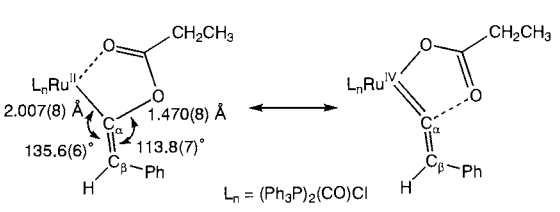

Scheme 3. Two resonance structures of the 1-propanoyloxy-2-phenylethenyl-C^1,O-chelate of **2a**.

distance (1.470(8) Å) falls within the range of those in [Ru(η^5-C_5H_5){C(=CHCO$_2$CH$_3$)OC(=O)CH$_3$}(PPh$_3$)] (1.493(2) Å) and [Ru{C(=CHPh)OC(=O)CH$_3$}-(CO)(acetone)(P^{i}Pr$_3$)$_2$]BF$_4$ (1.466(9) Å) and is ca. 0.1 Å longer than the C–O bond of the ethenyl ligand in [Ru(η^5-C_5H_5){C(=CHPh)O^{i}Pr}(CO)(PPh$_3$)]. The sp-like nature of C_α is responsible for the unusual bond angles in Ru–C27–C26 and O2–C27–C26. The value of the former (135.6(6)°) is larger and that of the latter (113.8(7)°) is smaller than 120° for an ideal sp^2 carbon.

The phenyl group on the C_β carbon is positioned *trans* to the ruthenium atom with respect to the exocyclic C=C bond, avoiding the steric hindrance of the two PPh$_3$ and the CO ligands. No spectroscopic and crystallographic evidence to support the presence of the *cis*-isomer was observed for **2a**. This is similar to the case of [Ru{C(=CHPh)OC(=O)CH$_3$}(CO)(acetone)-(P^{i}Pr$_3$)$_2$]BF$_4$ where the phenyl substituent on the C=C bond is situated *trans* to the ruthenium, and is quite contrasting with the fact that the sterically less demanding [Ru(η^5-C_5H_5){C(=CHCO$_2$CH$_3$)OC(=O)CH$_3$}(PPh$_3$)] is observed as a mixture of the *cis*- and *trans*-isomers at the C=C bond. Moreover, the CO$_2$CH$_3$ group of the 1-acetoxy-2-methoxycarbonylethenyl ligand is laid dominantly *cis* to the CpRu moiety.

3.3. C–O bond forming steps between the propanoate and alkyne moieties

As figured in the structure **B** in Scheme 3, the formation of the C–O bond is interpreted as a result of the nucleophilic attack of the carboxylate oxygen onto the C_α carbon of the ethenylidene ligand. Once the ethenylidene ligand is formed on the ruthenium center, the nucleophilic attack follows. Electron deficiency and electrophilicity at the C_α of the ethenylidene ligand are wel described in the literature [23]. Although the nucleophilicity of the carboxylate is somewhat weak, the chelation of the ligand stabilizes the resulting five-membered metallacycle. The long C27–O2 bond length may reflect the weak nucleophilicity of the coordinating carboxylate.

Reaction of **1** with PhC≡CD (phenylacetylene-d_1) gave only 2-deutero-1-propanoyloxy-2-phenylethenylruthenium(II) complex (**2a**-d_1). The terminal D completely moved onto the C_β of the ligand. This result shows apparently that the source of the β-hydrogen of the chelating ligand is the terminal hydrogen of the alkyne. On the basis of this finding, two possible pathways are illustrated in Scheme 4, according to the published mechanisms. One route includes a ruthenium-assisted direct 1,2-hydrogen shift from the C_α to the C_β of the terminal alkyne. This process is often found in octahedral d^6 complexes [24]. The other route is β-protonation of an alkynyl intermediate derived from the terminal alkyne. Both mechanisms require a

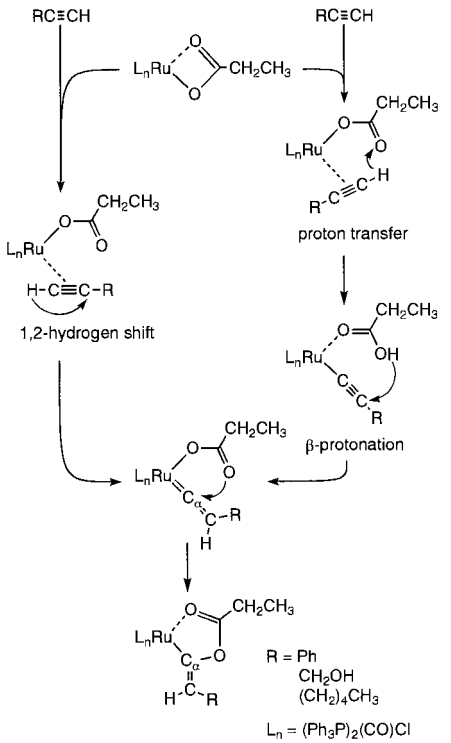

Scheme 4. Two possible routes for the (*Z*)-enol ester-like chelate ligand.

cleavage of the terminal C–H bond of the alkyne, being consistent with the inertness of the internal alkynes to the formation of the enol ester-like ligands.

In the former route, the C_α of the resulting ethenylidene ligand is attacked successively by the coordinating carboxylate nucleophilically. The carboxylate ligand need not be released from the ruthenium throughout the formation of the chelate. In the latter route, carboxylic acid, from the coordination sphere, is a real source of the proton, therefore the proton attached to the terminal alkyne should be transferred to the carboxylate residue to release the free carboxylic acid in contrast to the former route. Therefore the latter route is practically impossible because of the acidity of the terminal alkyne is too weak to liberate the free carboxylic acid from the carboxylate complex.

3.4. Acidolysis of **2a** and ruthenium complex-catalyzed (*Z*)-enol ester-selective synthesis

The (*Z*)-enol ester-like backbone of the 1-propanoyloxy-2-phenylethenyl-C^1,O ligand suggests directly that complex **2a** is a possible catalyst for the (*Z*)-enol ester-selective addition of propanoic acid to phenylacetylene. As stated above, the propanoate complex **1** readily reacts with phenylacetylene to give **2a**. If **2a** reacts successively with propanoic acid to liberate (*Z*)-2-phenylethenyl propanoate and to reproduce **1**, a catalytic cycle is completed to produce the (*Z*)-enol ester selectively (see (*Z*)-enol ester manifold in Scheme 5).

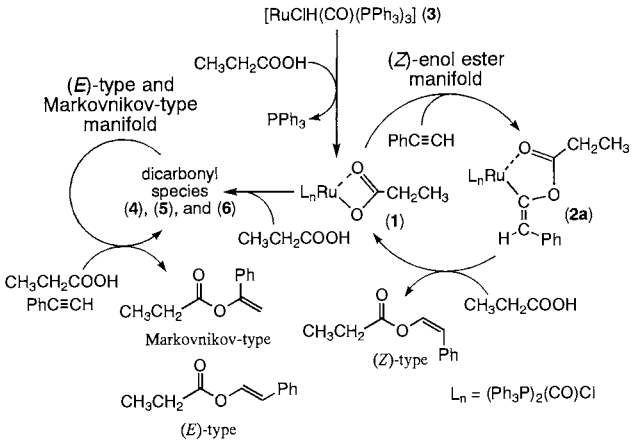

Scheme 5. The catalytic cycles for the selective addition of propanoic acid to phenylacetylene.

Therefore the following detailed analysis of the acidolysis of **2a** is examined.

Treatment of **2a** with propanoic acid in refluxing benzene gave (*Z*)-2-phenylethenyl propanoate; the *cis*-geometry between the phenyl group and the propanoyloxy group was retained in the acidolysis. The production of the (*Z*)-enol ester through the acidolysis of **2a** implies that the ruthenium complex-catalyzed synthesis of the enol ester can proceed via **2a**. Nevertheless, it should be noted that the acidolysis of **2a** does not completely reproduce the propanoate **1**. The ^{31}P-NMR spectrum of the reaction mixture showed not only the signal of **1** (δ 34.4) but additional three singlets at δ 31.8, 24.1 and 15.4. These three singlets were assigned to a dicarbonylbis(η^1-propanoato) complex [Ru{η^1-OC(=O)C_2H_5}$_2$(CO)$_2$(PPh_3)$_2$] (**4**), and to a dicarbonylchloro(η^1-propanoato) complex [RuCl{η^1-OC(=O)C_2H_5}(CO)$_2$(PPh_3)$_2$] (**5**), and to a dicarbonyldichloro complex *cct*-[$RuCl_2$(CO)$_2$(PPh_3)$_2$] (**6**) [14], respectively. The relative ratio of **1** based on the integrated ^{31}P peak area fell only 20% when the acidolysis was completed. The relative ratios of three dicarbonyl species were 14% for **4**, 50% for **5**, and 16% for **6**. The amounts of **4** and **6** were almost equal to each other during the acidolysis. Apparently, formation of the bis(propanoato) and the dichloro complexes **4** and **6** should be a result of disproportionation of the chloropropanoato complex **5**. The acidolysis of **2a** giving the (*Z*)-enol ester and the dicarbonylchloro(η^1-propanoato) complex **5** is very similar to those of the neutral [RuCl{C(=CHPh)OC(=O)CH_3}(CO)(P^iPr_3)$_2$] and the cationic [Ru{C(=CHPh)OC(=O)CH_3}(CO)(acetone)-(P^iPr_3)$_2$]$^+$ reported by Esteruelas et al. [11]. The source of the second carbonyl of these complexes seems to be the carboxylic acid. There are some examples of the ruthenium complexes-promoted decarbonylation of organic acids and esters although detail of its process is unknown [25].

The liberation of the (*Z*)-enol ester in the acidolysis of the complex **2a** prompted us to try the addition of propanoic acid to phenylacetylene catalyzed by **2a**. In order to compare the catalytic activity and selectivity, the propanoato complex **1** and a hydridoruthenium(II) complex [RuClH(CO)(PPh_3)$_3$] (**3**) were also used as a catalyst or a catalyst precursor. Table 2 summarizes the results of the catalytic addition. When **1** or **2a** was used as a catalyst precursor, the total yield of the enol esters reached up to 99% within 24 h in refluxing benzene and no dimer of phenylacetylene (diphenylbut-1-en-3-ynes) that was often formed in the presence of a transition-metal complex-catalyst [26] was recognized. As for the selectivity, 1-phenylethenyl propanoate was formed together with (*Z*)-2-phenylethenyl propanoate preferentially. On the other hand, catalytic addition using **3** as a catalyst precursor was much slower than those using **1** and **2a**; it afforded the enol esters in only 35% yield after 72 h accompanied by a small amount of the dimers. The rest of the acid and alkyne remained non-reacted. Among the three isomers of the enol ester, the (*Z*)-type was produced in 86% relative selectivity using **3**. Very interestingly, the presence of the additional PPh_3 (run 2) suppressed the total yield of the enol esters but increased the relative selectivity for the (*Z*)-type enol ester up to 86% compared to those in the run 1. These results are the third example of selective (*Z*)-enol ester formation catalyzed by a ruthenium complex following Dixneuf's catalytic system [8], but are in contrast to the case of the ferrocenecarboxylato complex [Ru{η^2-$O_2C(C_5H_4)Fe(C_5H_5)$}Cl(CO)(PPh_3)$_2$] that has been shown to be a very effective catalyst precursor

Table 2
Addition of propanoic acid to phenylacetylene catalyzed by ruthenium complexes

Reaction				Relative ratio (%)		
Run	Complex	Time (h)	Yield (%)	(*Z*)-type	(*E*)-type	Markovnikov-type
1	**1**	24	>99	35	7	58
2	**1** [a]	72	29	86	4	10
3	**2a**	24	>99	42	7	51
4	**3**	72	35	86	9	5

[a] Triphenylphosphine was added: [PPh_3]/[Ru] = 1.0.

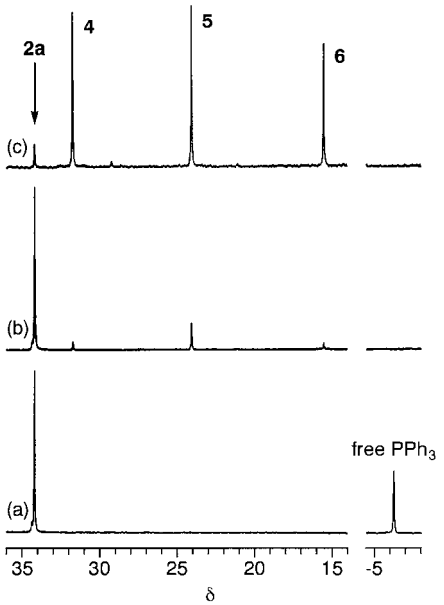

Fig. 2. The $^{31}P\{^{1}H\}$-NMR spectra of the ruthenium species in the catalytic addition of propanoic acid to phenylacetylene: (a) complex, **3**; reaction time, 0.5 h; (b) complex, **1**; reaction time, 0.5 h; (c) complex, **1**; reaction time, 15 h. These spectra were observed in C_6D_6; the ^{31}P-chemical shift value of **2a** (δ 34.3) is slightly different from that in $CDCl_3$ (δ 33.6).

in the (*Z*)-selective addition of ferrocenecarboxylic acid to phenylacetylene [9].

The ^{31}P-NMR spectra of the catalytic reaction mixtures are shown in Fig. 2. When **3** was employed for the catalyst precursor, the ^{31}P-signals of **3** completely turned into those of **2a** and free PPh_3 within 30 min despite the slow formation of the enol esters. Once **2a** appeared, any other ruthenium-containing species (the propanoate **1**, the starting **3** complex, and the dicarbonyl species **4**, **5**, and **6**) was not observed throughout the catalytic reaction. The presence of **2a** as the only observable complex apparently means the acidolysis of **2a** is the rate-determining step of the catalytic cycle. When **1** was used for the catalyst, in contrast, the starting complex **1** disappeared within 30 min. The reaction mixture contained **2a** and three dicarbonylruthenium species **4**, **5**, and **6**. The complex **2a** also disappeared when the catalytic reaction was completed, and there remained only **4**, **5**, and **6**. When **2a** was used for the catalyst precursor, the results were similar to those for **1**. The use of **3** means the presence of the excess free PPh_3 in the catalytic mixture. In the presence of the excess free PPh_3, even **1** afforded the complex **2a** and the (*Z*)-enol ester; the formation of **4**, **5**, and **6** was suppressed. In other words, the presence of the free PPh_3 effectively suppresses the competitive side-reaction leading to the dicarbonylruthenium species **4**, **5**, and **6**.

3.5. Conclusions: the intermediates in the catalysis and the origin of the (Z)-enol ester-selectivity

The results of the acidolysis and the catalytic reactions indicate that the (*Z*)-enol ester is produced predominantly by the acidolysis of **2a** in the catalytic cycle. The presence of free PPh_3 in the catalytic system leads the predominant formation of **2a** from **1** and phenylacetylene. After all, the presence of the free PPh_3 causes the (*Z*)-selectivity in the catalysis. The most plausible (*Z*)-selecting mechanism is as the followings: the slow acidolysis of **2a** by propanoic acid gives the (*Z*)-enol ester and the propanoato complex **1**. Once the complex **1** is produced, it is converted competitively into **2a** or the three dicarbonyl species **4**, **5**, and **6** under the reaction conditions. When the free PPh_3 is present in the reaction mixture, PPh_3 suppresses the competitive formation of the dicarbonyl species. Therefore, the two intermediary species, **1** and **2a** complete the catalytic cycle producing the (*Z*)-enol ester. In the absence of the free PPh_3, the dicarbonyl species evolve after the acidolysis, bring about another catalytic route including them, and lead the production of the (*E*)- and Markovnikov-type enol esters. As stated here, the structure of the intermediate **2a** and the origin of the (*Z*)-selectivity of the catalytic system are clearly rationalized in this study.

4. Supplementary material

Crystallographic data for the structural analysis have been deposited with the Cambridge Crystallographic Data Centre, CCDC no. 113479 for **2a**·$2CH_2Cl_2$. Copies of this information may be obtained free of charge from: the Director, CCDC, 12 Union Road, Cambridge, CB2 1EZ, UK (Fax: +44-1223-336033; e-mail: deposit@ccdc.cam.ac.uk or WWW: http://www.ccdc.cam.ac.uk).

Acknowledgements

A part of this work was financially supported by a grant for one of the authors (H.K.) from the Foundation 'Hattori-Hokokai.'

References

[1] (a) T. Mitsudo, Y. Hori, Y. Watanabe, J. Organomet. Chem. 334 (1987) 157. (b) C. Bruneau, P.H. Dixneuf, Chem. Commun. (Cambridge) (1997) 507 and references cited therein.

[2] (a) T. Mitsudo, Y. Hori, Y. Watanabe, J. Org. Chem. 50 (1985) 1566. (b) T. Mitsudo, Y. Hori, Y. Yamanaka, Y. Watanabe, Tetrahedron Lett. 27 (1986) 2125. (c) T. Mitsudo, Y. Hori, Y. Watanabe, J. Org. Chem. 52 (1987) 2230.

[3] (a) C. Ruppin, P.H. Dixneuf, Tetrahedron Lett. 27 (1986) 6323. (b) C. Ruppin, P.H. Dixneuf, S. Lécolier, Tetrahedron Lett. 29 (1988) 5365.
[4] K. Philippot, D. Devanne, P.H. Dixneuf, J. Chem. Soc. Chem. Commun. (1990) 1199.
[5] M. Neveux, C. Bruneau, P.H. Dixneuf, J. Chem. Soc. Perkin Trans. 1 (1991) 1197.
[6] M. Neveux, B. Seiller, F. Hagedorn, C. Bruneau, P.H. Dixneuf, J. Organomet. Chem. 453 (1991) 133.
[7] M. Rotem, Y. Shvo, J. Organomet. Chem. 448 (1993) 189.
[8] (a) H. Doucet, J. Höfer, C. Bruneau, P.H. Dixneuf, J. Chem. Soc. Chem. Commun. (1993) 850. (b) H. Doucet, B. Martin-Vaca, C. Bruneau, P.H. Dixneuf, J. Org. Chem. 60 (1995) 7247.
[9] L. Matas, I. Moldes, J. Soler, J. Ros, Á. Alvarez-Larena, J.F. Piniella, Organometallics 17 (1998) 4551.
[10] T. Daniel, N. Mahr, T. Braun, H. Werner, Organometallics 12 (1993) 1475.
[11] M.A. Esteruelas, F.J. Lahoz, A.M. López, E. Oñate, L.A. Oro, Organometallics 13 (1994) 1669.
[12] N. Ahmad, J.J. Levison, S.D. Robinson, M.F. Uttley, Inorg. Synth. 15 (1974) 45.
[13] (a) S.D. Robinson, M.F. Uttley, J. Chem. Soc. Dalton Trans. (1973) 1912. (b) K. Hiraki, A. Nonaka, T. Matsunaga, H. Kawano, J. Organomet. Chem. 574 (1999) 121.
[14] D.W. Krassowski, J.H. Nelson, K.R. Brower, D. Hauenstein, R.A. Jacobson, Inorg. Chem. 27 (1988) 4294.
[15] A. Dobson, S.D. Robinson, M.F. Uttley, Inorg. Synth. 17 (1977) 124.
[16] F. Hai-Fu, SAPI-91, Structure Analysis Programs with Intelligent Control, Rigaku Corporation, Tokyo, Japan, 1991.
[17] P.T. Beurskens, G. Admiraal, G. Beurskens, W.P. Bosman, S. Garcia-Granda, R.O. Gould, J.M.M. Smits, C. Smykalla, DIRDIF-92, The DIRDIF Program System, Technical Report of the Crystallography Laboratory, University of Nijmegen, The Netherlands, 1992.
[18] TEXSAN, Crystal Structure Analysis Package, Molecular Structure Corporation, 1985, 1992.
[19] M.I. Bruce, D.N. Duffy, M.G. Humphrey, A.G. Swincer, J. Organomet. Chem. 282 (1985) 383.
[20] J. López, A. Romero, A. Santos, A. Vegas, A.M. Echavarren, P. Noheda, J. Organomet. Chem. 373 (1989) 249.
[21] A. Romero, A. Santos, A. Vegas, Organometallics 7 (1988) 1988.
[22] R. Le Lagadec, E. Roman, L. Toupet, U. Müller, P.H. Dixneuf, Organometallics 13 (1994) 5030 and references cited therein.
[23] (a) N.M. Kostic, R.F. Fenske, Organometallics 1 (1982) 974. (b) H. Werner, J. Wolf, R. Zolk, U. Schubert, Angew. Chem. Int. Ed. Engl. 22 (1983) 981. (c) H. Werner, J. Wolf, G. Müller, C. Kruger, Angew. Chem. Int. Ed. Engl. 23 (1984) 431.
[24] (a) M.I. Bruce, Chem. Rev. 91 (1991) 197. (b) Y. Wakatsuki, N. Koga, H. Yamazaki, K. Morokuma, J. Am. Chem. Soc. 116 (1994) 8105.
[25] (a) J. Ropp, J. Am. Chem. Soc. 82 (1960) 842. (b) T. Yamamoto, S. Miyashita, Y. Naito, S. Komiya, T. Ito, A. Yamamoto, Organometallics 1 (1982) 808. (c) K. Hiraki, S. Kira, H. Kawano, Bull. Chem. Soc. Jpn. 70 (1997) 1583.
[26] R. Mahé, P.H. Dixneuf, S. Lécolier, Tetrahedron Lett. 27 (1986) 6333.